Contemporary Engineering Sciences, Vol. 16, 2023, no. 1, 55 - 70
HIKARI Ltd, www.m-hikari.com
https://doi.org/10.12988/ces.2023.93115

Smart Agriculture: Predictive Height Analysis for Universal Crop Health Classification

Sotirios Tsakiridis, Nikolaos Papaioannou, Alkiviadis Tsimpiris, Dimitrios Varsamis

Department of Computer, Informatics and Telecommunications Engineering
International Hellenic University
Serres, 62100, Greece

Apostolos Papakonstantinou

Department of Civil Engineering and Geomatics
School of Engineering and Technology
Cyprus University of Technology
Limassol, 3036, Cyprus

Abstract

The use of contemporary information and communication technology to maximize agricultural output while reducing labor costs is known as "smart agriculture". This term is becoming more and more prevalent. The primary challenge in the agricultural sector lies in the vastness of crops, coupled with varied topography and soil instability, making control challenging. In this paper, a system for determining the average predicted height of healthy plants at a given growth stage is proposed and evaluated. Based on this height, we then classify agricultural plants as healthy or unhealthy. It's important to note that our system works with any crop kind and growth stage.

Keywords: Smart Agriculture, Unmanned Aerial Vehicles, Clustering, Unsupervised Learning

1 Introduction

In the ever-evolving landscape of agriculture, the integration of cutting-edge technologies has ushered in a new era of efficiency and precision Smart Agriculture. As global populations burgeon, the demand for sustainable and high-yielding crop production intensifies, [19]. Smart Agriculture, empowered by innovative technologies and data-driven methodologies, emerges as a transformative solution to address these challenges, [20], [14], [5], [2], [4]. Modern technology has significantly contributed to the improvement of various industrial sectors, including agriculture. In the field of agriculture, it has provided solutions to often time-consuming and labor-intensive tasks, fundamentally altering the way we perceive agricultural production, [15], [10], [6], [16]. The essence of Smart Agriculture lies in its ability to not only streamline traditional practices but also address key factors that often lead to reduced yields and compromised product quality. Key factors leading to reduced yields and diminished product quality include plant infestations by pests and diseases, [11], nutrient deficiencies, as well as the growth of weeds competing with plants for nutrients and water. All of the above result in the alteration of the external appearance of plants, primarily hindering their growth and causing discoloration of plant parts.

The alteration in the plants as a result of the aforementioned external factors does not manifest uniformly throughout the entire cultivation. Instead, it initially appears in isolated and often non-adjacent areas in the form of irregular "spots", that progressively spread throughout the entire cultivation. Therefore, the detection of these problematic areas at an early stage, [9], is imperative to address them promptly using chemical, biological, or other methods, thereby minimizing production loss and consequently mitigating the reduction in farmers' income.

Detecting all these problematic areas in large expanses is particularly challenging, especially in crops with tall plant heights (such as corn, sunflowers, etc.) where ground-based methods are impractical, [7]. A panoramic capture is required to identify areas with plant heights lower than expected, based on the specific stage of their development. Therefore, the semantic segmentation of the field represents the first and most crucial stage in effectively addressing and limiting the spread of "diseased" plants, [3].

Smart Agriculture leverages an array of methods to monitor and optimize crop performance. Remote sensing technologies, such as satellite imagery, [21], and aerial drones, [17], [7], provide a bird's-eye view of agricultural landscapes, enabling farmers to assess crop health, detect anomalies, [13], and make informed decisions. In addition, in recent agricultural research, advanced technologies such as convolutional neural networks, [12], and LiDAR scanners have been also employed in plant analysis, [18], [1]. These tools, combined with data

analytics, facilitate real-time monitoring and timely interventions. However, most of the studies specialize in specific types of crops (agroforestry, vegetables, etc.) and address specific challenges related to these cultivations. Additionally, the proposed methodologies incur high computational costs and cannot be applied in real-time.

The primary objective of this work is to study and implement a unified computational model for identifying problematic areas in large-scale cultivations (agroforestry, cereals, industrial plants, medicinals, etc.) without prior knowledge of the crop type or the stage of plant growth. The problem is approached incrementally, starting from smaller to larger scales, using a field simulator with problematic areas developed in the Python language.

The rest of the paper is structured as follows: Section 2 introduces the fundamental elements of the theory and methodology employed. Section 3 presents the results of the comparative study and finally, Section 4 offers the discussion and the conclusions..

2 Materials and Methods

As previously mentioned, the primary objective of this study is to implement a unified computational model for identifying problematic areas in large-scale cultivations without prior knowledge of the crop type or the stage of plant growth. To achieve this, LIDAR was employed for data acquisition. Initially, a sampling of the cultivation is conducted with predetermined frequencies along both the length and width. Under simulation conditions, the maximum possible resolution was utilized (1 pixel per unit length). Subsequently, three interpolation techniques (Flat, Half Flat, and Linear) are applied to regenerate the cultivation from the sampled points, enabling a close approximation of the actual situation. This approach allows real-time reshaping with simultaneous interpolation during the sampling point acquisition. Data processing occurs during the flight through a controller adapted to the aerial vehicle. Finally, criteria for the rapid detection of problematic areas are explored, involving the calculation of a height threshold for plants. Specifically, it is explained how the threshold is applied to distinguish healthy and unhealthy plants in the regenerated field. The research utilizes a UAV model with tilted rotors and an ArduPilot controller for data collection, with a Raspberry Pi serving as the microcontroller for data processing. Figure 1 depicts the three fundamental stages of the computational process.

Figure 1: Project Flowchart.

2.1 Interpolation techniques

2.1.1 Flat interpolation

In flat interpolation, the sampled value is extended to all intermediate points between two sampled positions. In simpler terms, if $f(a)$ and $f(b)$ represent consecutive sampled values at points a and b along the flight direction, every midpoint between them assumes the value of $f(a)$. This can be succinctly expressed as:

$$\forall c \in (a, b) : f(c) = f(a)$$

2.1.2 Half flat interpolation

In half flat interpolation, the midpoints receive the value $f(a)$, and the remaining ones receive the value $f(b)$:

$$\forall c_1 \text{ with } a < c_1 \leq a + \left\lceil \frac{b-\alpha}{2} \right\rceil : f(c) = f(a)$$

$$\forall c_2 \text{ with } a + \left\lceil \frac{b-\alpha}{2} \right\rceil < c_2 < b : f(c) = f(b)$$

2.1.3 Linear interpolation

In linear interpolation, a smooth transition is made from the value $f(a)$ to the value $f(b)$. If there are n points between a and b (depending on the sampling

frequency), we define the step increase step as follows:

$$\text{step} = \frac{f(b) - f(a)}{n}$$

and values are assigned as follows:

$$\forall c_i \text{ with } \alpha < c_i \leq b, 1 \leq i \leq n : f(c_i) = f(c_{i-1} + i \cdot \text{step})$$

2.2 Equipment

For the research needs, a UAV model with tilted rotors and an ArduPilot controller, [8], have been utilized. In these UAVs (drones), the rotors are positioned on wings and can tilt between vertical and horizontal positions. In the vertical mode, they function like a helicopter, allowing vertical takeoff and landing. In the air, the rotors can tilt into a horizontal position, enabling the UAV to fly like a fixed-wing aircraft.

A Raspberry Pi (version 3) was used as the microcontroller for data collection and processing. This model is essentially a microcomputer with an ARM Cortex-A53 SoC processor and 1GB RAM. It features interfaces for attaching external devices and sensors. These interfaces facilitate the connection with the ArduPilot microcontroller of the UAV.

3 Results and Discussion

This research focuses on the following points:

a. Criteria for accurate cultivation mapping:

- Determining the optimal sampling rate (drone speed) and the best flight path for collecting the required data.
- Identifying the optimal algorithm for real-time mapping.

b. Criteria for rapid detection of problematic areas:

- Finding the optimal recording rate (drone speed) and the best (shortest time) flight for sampling.
- Identifying the best (in terms of execution speed and computational simplicity) algorithm for real-time mapping.

In order to accomplish this, crop simulations covering an area of 40,000 square meters, including specific problematic areas, were generated. The simulation was conducted for three distinct cases.

In this section, we present a comprehensive analysis of the results obtained from the simulation. The focus will be on one of the three cases, with a subsequent summary of findings across all scenarios. Figure 2 illustrates a 3D rendering of the simulated crop. The green color denotes the healthy portion of the crop, whereas the yellow indicates areas where the crop has not grown properly. Two problematic areas are evident in the illustration. The smaller of the two is situated in the left part, approximately in the middle of the field, while the larger one is located in the lower-left part of the field.

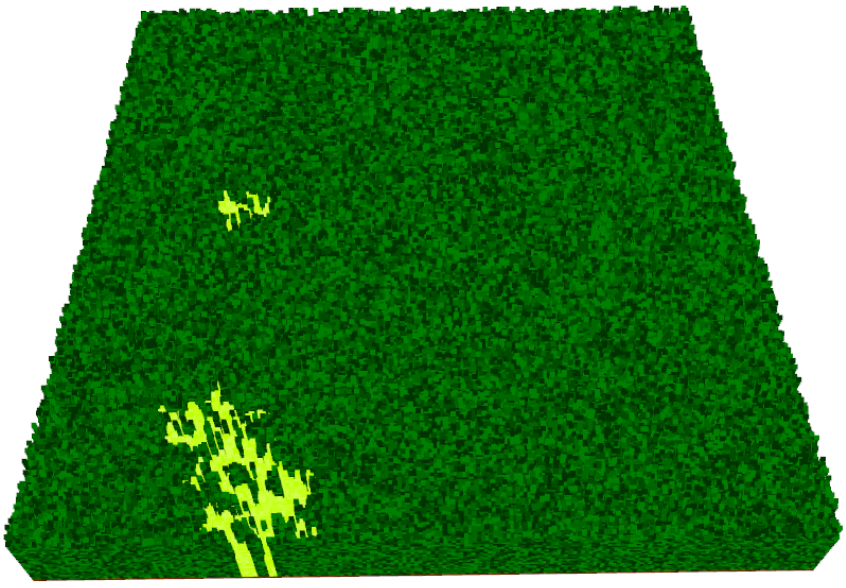

Figure 2: 3D rendering of the crop.

Figure 3 illustrates the actual crop simulation, showcasing plant heights and highlighting areas with issues.

We observe that across the entire field, the plants exhibit a height equal to or greater than 20. However, in the lower-left and left-middle sections, there are noticeable regions where plant development is less robust (indicated by the pink-orange areas). In these specific zones, some plants have a height ranging from 10 to 15, significantly lower than the general field average. The goal is to capture the field and identify areas (if any) where issues are present, and plants have not developed as expected. To achieve this objective, a variety of methodologies have been explored in the existing literature.

One approach to capturing the development of a cultivation involves the application of remote sensing and machine learning methodologies. A draw-

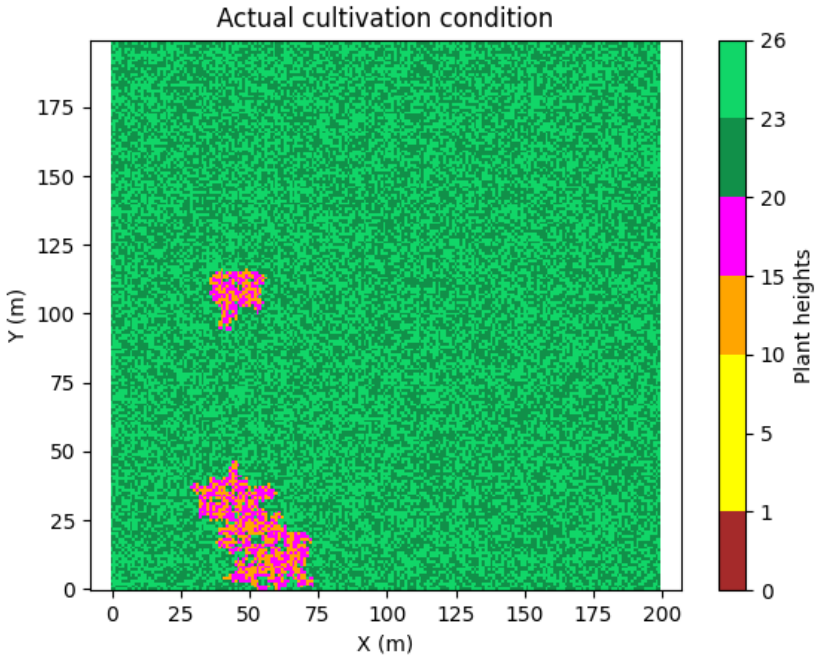

Figure 3: Crop Simulation: Troubled Areas.

back of this method is that the flight must be completed before data processing can occur, rendering it unsuitable for real-time use. Moreover, this approach does not provide the capability to monitor field issues in real-time. To address this limitation, we adopt an alternative strategy. Instead of conducting a comprehensive survey across the entire field, we opt for a sampling method. In this particular study, we employ a data acquisition technique using LIDAR. Initially, a sampling of the cultivation is conducted with predetermined frequencies along both the length and width. The highest resolution (1 pixel per unit length) was utilized. The outcomes of this sampling are depicted in Figure 4.

Subsequently, three interpolation techniques are applied to regenerate the cultivation from the sampling points. In particular, the Flat interpolation, Half Flat interpolation and Linear interpolation methods, which were examined in Sections 2.1.1, 2.1.2, and 2.1.3, respectively. The results of the interpolation are illustrated in Figures 5, 6 and 7.

We observe that Half Flat and Flat interpolations exhibit almost identical results, while Linear interpolation slightly differs in plant height determinations. Nevertheless, in all three interpolation cases, the regeneration of the field from the sampling points closely approximates the actual situation (Fig. 1), and problematic areas are precisely identified. This approach enables real-time

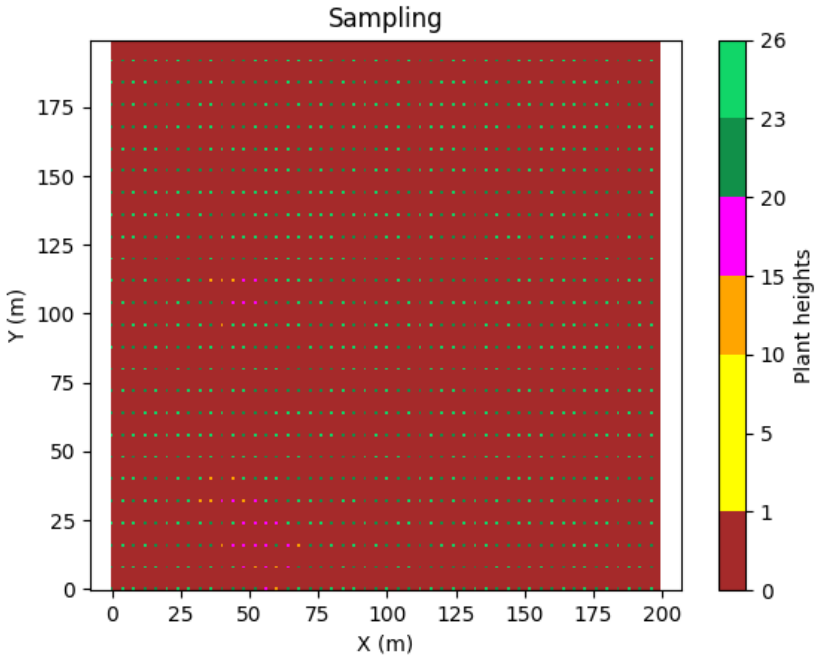

Figure 4: Sampling result.

reshaping with simultaneous interpolation during the acquisition of sampling points. Data processing occurs during the flight through a controller adapted to the aerial vehicle. It is noteworthy that the computational complexity in all three interpolation methods is minimal.

To identify problematic areas, it is essential to calculate a height threshold for plants. Points with values above this threshold are classified as belonging to healthy plants, while those below it are considered unhealthy. Initially, the points from the regenerated field through interpolation are grouped after normalizing the values to the nearest integer. Figure 8 visually represents the distribution of points in a frequency histogram.

Visually, it is apparent that points with a height value exceeding 20 units correspond to healthy plants, whereas those below 20 units indicate unhealthy ones. The red line in the graph signifies the mean value between the maximum and minimum values of the classes. The threshold value is established as the first class with a frequency exceeding this mean value. Consequently, in Figure 8, the threshold value is determined to be 20.

Upon applying the threshold to the points of the regenerated field through sampling, specifically in the case of flat interpolation, the resulting representation is depicted in Figure 9. Put simply, every height value surpassing 20 is deemed indicative of a healthy plant and is visually represented in green,

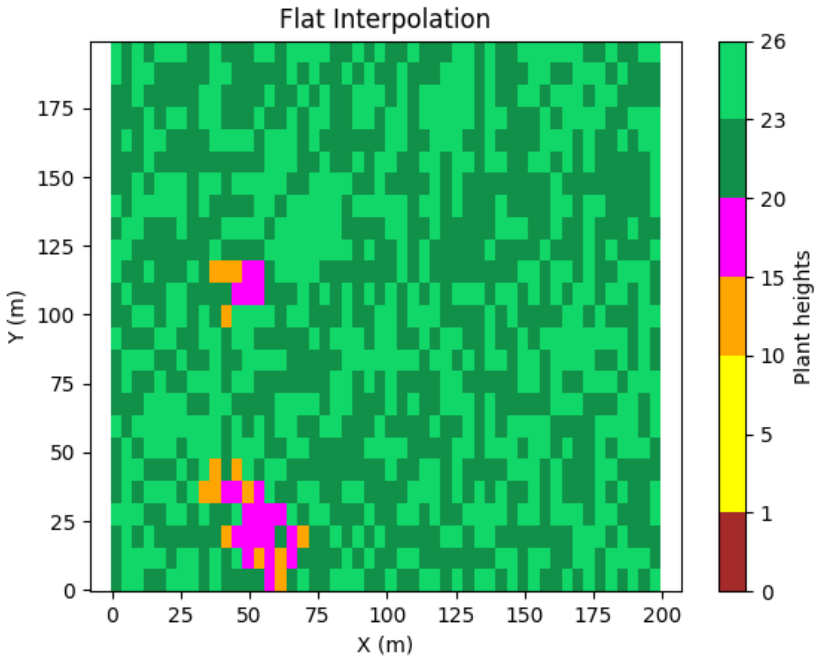

Figure 5: Flat interpolation.

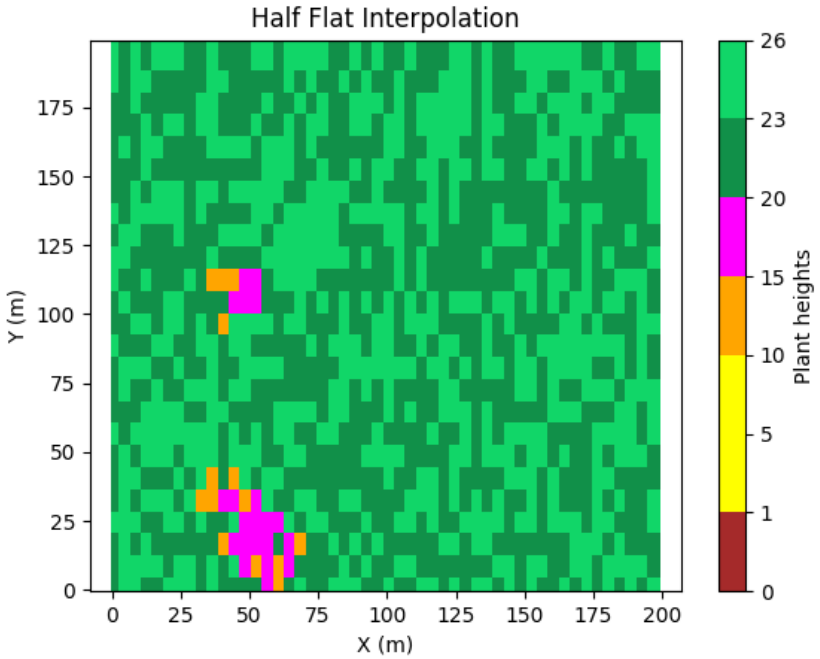

Figure 6: Half Flat interpolation.

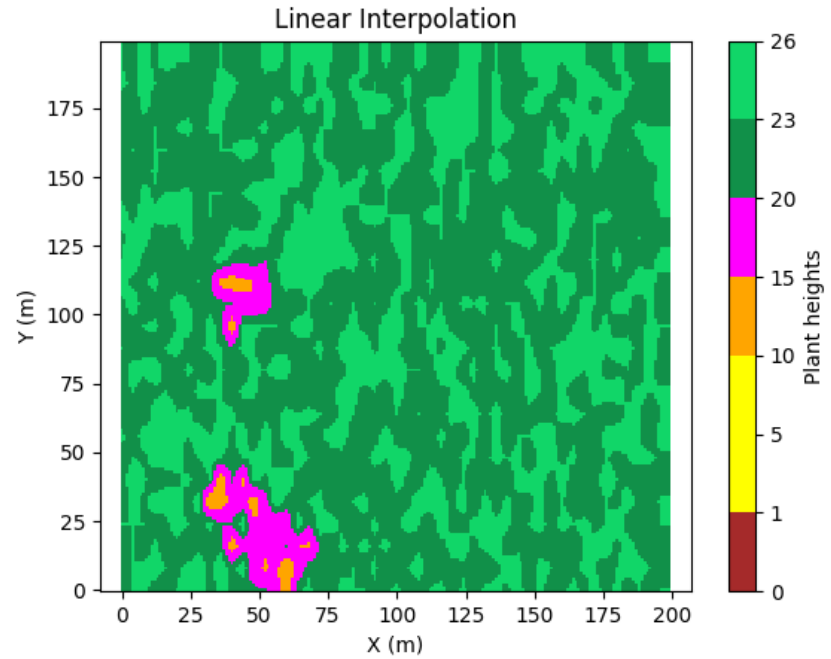

Figure 7: Linear interpolation.

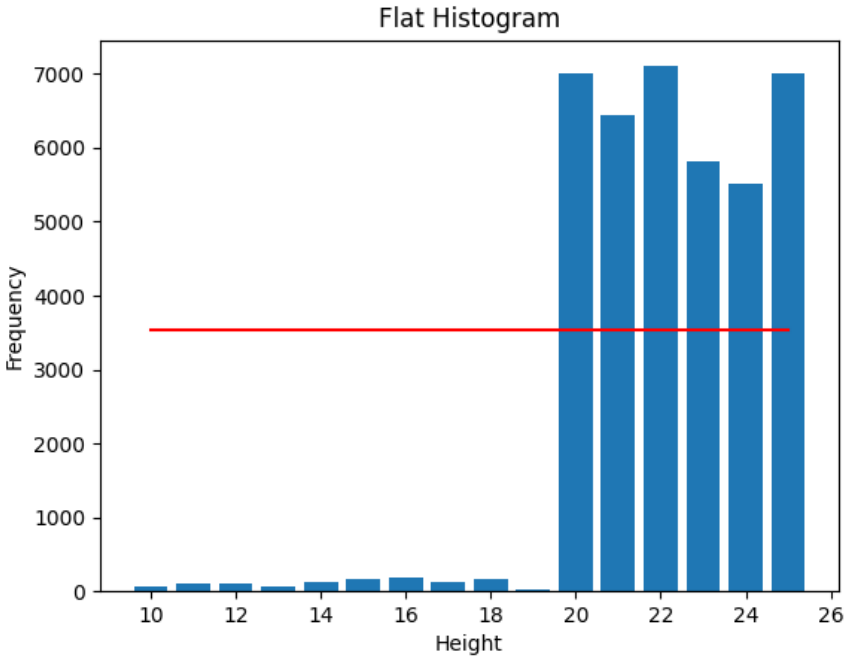

Figure 8: Frequency Distribution of Plant Height.

while all points registering a height below 20 are identified as diseased plants, visualized in yellow. Conventionally, if t represents the threshold value and $f(x, y)$ denotes the height of the point at position (x, y) within the field, the threshold function g is succinctly defined as follows:

$$g(x,y) = \begin{cases} 1 & \text{if } f(x,y) \geq t \\ 0 & \text{if } f(x,y) < t \end{cases}$$

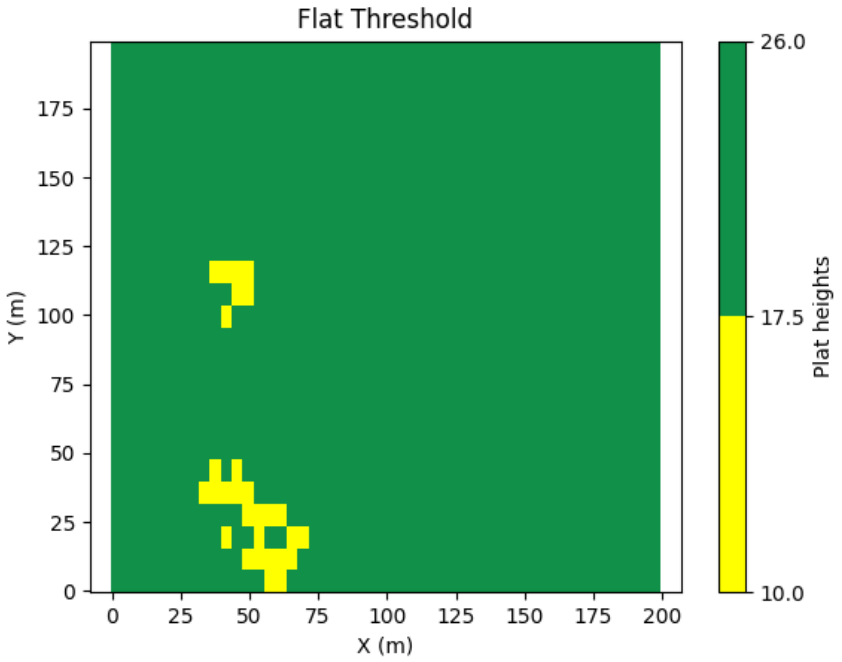

Figure 9: Threshold application.

For the remaining two cases under investigation, the outcomes and resulting conclusions align closely with the outcomes and subsequent conclusions of the initial case. In the interest of efficiency, and to conserve both time and space, we opt not to provide an exhaustive presentation. Within each case, concise graphical representations are presented which showcase actual crop, sampling result, flat, half-flat and linear interpolation and the associated threshold application. Figures 9 and 10 provide a succinct portrayal of these elements for Cases 2 and 3, respectively.

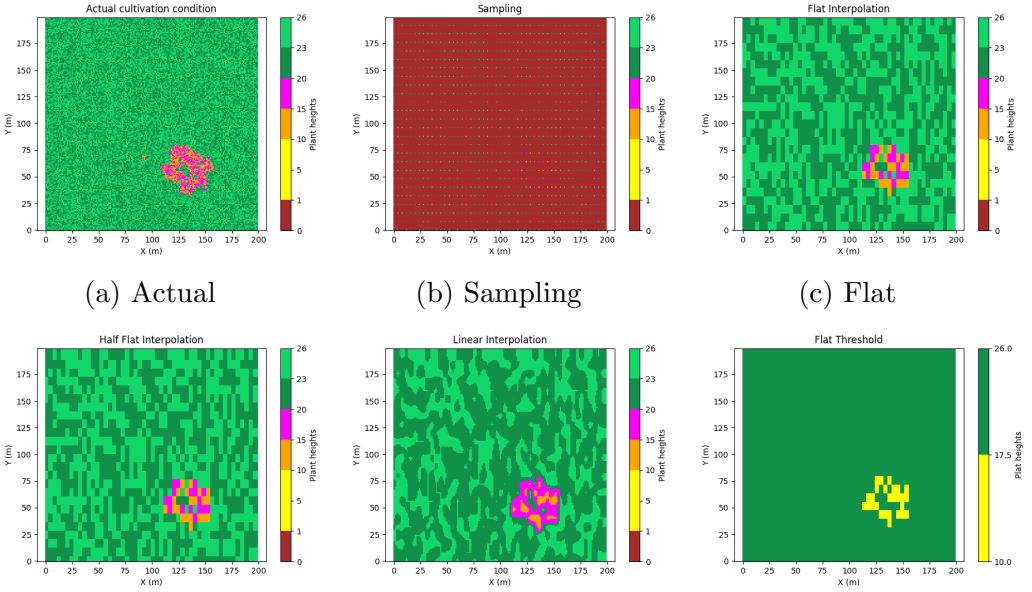

(a) Actual (b) Sampling (c) Flat

(d) Half-Flat (e) Linear (f) Threshold

Figure 10: Graphical representations illustrating actual crop, sampling results, flat, half-flat, and linear interpolation, along with threshold application.

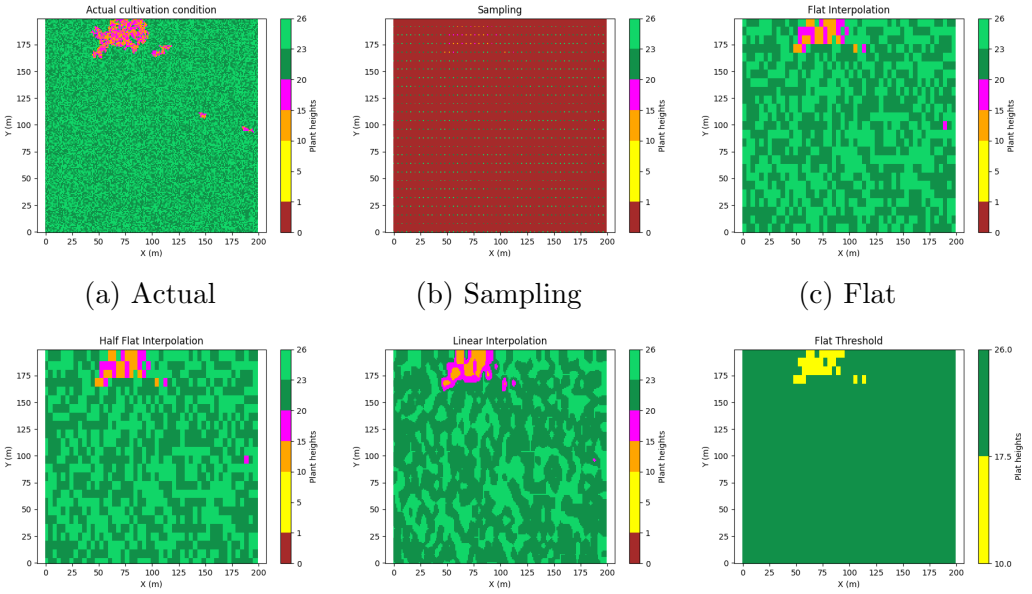

(a) Actual (b) Sampling (c) Flat

(d) Half-Flat (e) Linear (f) Threshold

Figure 11: Graphical representations illustrating actual crop, sampling results, flat, half-flat, and linear interpolation, along with threshold application.

4 Conclusion

Building upon the earlier analysis, our study demonstrates that the identification of problematic areas in crop fields, particularly under simulation conditions, achieves a remarkable level of precision. The significance of this precision lies in its potential to enable early detection and intervention, providing producers with a valuable tool to address compromised crop growth. The proactive approach facilitated by this methodology not only safeguards against potential income reduction but also contributes to the overall health and productivity of the cultivation.

The low computational complexity in this methodology enhances its practicality for real-time implementation. The ability to operate in real-time, coupled with suitability for parallel execution, ensures that the methodology is not only effective but also efficient. Producers can seamlessly integrate this approach into their cultivation practices, allowing for continuous monitoring and timely interventions.

Our findings highlight the methodology's robustness, as it offers a comprehensive solution for precision agriculture. The integration of sampling techniques, LIDAR technology, and interpolation methods allows for the accurate regeneration of the field, enabling producers to visualize and address problematic areas with precision. This integrative approach empowers producers with timely insights, fostering proactive decision-making for optimal cultivation management.

In conclusion, our study provides an efficient methodology for monitoring and managing crop fields. By combining technological advancements and computational methods, we offer a solution that not only identifies problematic areas accurately but also facilitates real-time interventions. The proactive nature of this approach positions it as a valuable tool for producers, contributing to the sustainability and efficiency of modern agriculture practices.

Acknowledgements. This research was carried out as part of the project 'Development of Smart Agriculture Applications for monitoring- production improvement and training of farmers' (Project code: KMP6-0086976) under the framework of the Action 'Investment Plans of Innovation' of the Operational Program 'Central Macedonia 2014 2020', that is co-funded by the European Regional Development Fund and Greece.

References

[1] T. Adams, R. Bruton, H. Ruiz Guzman, I. Perez, M. G. Selvaraj, and D. Hays, Prediction of aboveground biomass of three cassava (manihot

esculenta) genotypes using a terrestrial laser scanner, *Remote Sensing*, **13** (2021) 1272. https://doi.org/10.3390/rs13071272

[2] K. Avanidou, T. Alexandridis, D. Kavroudakis, and T. Kizos, Devel- opment of a multi scale interactive web-GIS system to monitor farmingpractices: A case study in lemnos island, Greece, *Smart Agricultural Technology*, **5** (2023), 100313. https://doi.org/10.1016/j.atech.2023.100313

[3] Y. Chen, Y. Xiong, B. Zhang, J. Zhou, and Q. Zhang, 3D point cloud semantic segmentation toward large-scale unstructured agricultural scene classification, *Computers and Electronics in Agriculture*, **11** (2021), 106445. https://doi.org/10.1016/j.compag.2021.106445

[4] Y. Chen, H. Zhu, and E. Ozkan, Real-time tree foliage density estimation with laser scanning sensor for variable-rate tree sprayer development, *American Society of Agricultural and Biological Engineers*, **3** (2013). https://doi.org/10.13031/aim.20131596009

[5] J. Cho, C. Kim, K.J. Lim, J. Kim, B. Ji, and J. Yeon, Web-based agri- cultural infrastructure digital twin system integrated with gis and BIM concepts, *Computers and Electronics in Agriculture*, **215** (2023). https://doi.org/10.1016/j.compag.2023.108441

[6] M. Gonzalez-de Soto, L. Emmi, M. Prez-Ruiz, Juan Agera V., and P. Gonzalez-de Santos, Autonomous systems for precise spraying evalua- tion of a robotised patch sprayer, *Biosystems Engineering*, **146** (2016), no. 1. https://doi.org/10.1016/j.biosystemseng.2015.12.018

[7] M. Hobart, M. Panz, C. Weltzien, and S. Michael, Growth height determination of tree walls for precise monitoring in apple fruit production using uav photogrammetry, *Remote Sensing*, **12** (2020), no. 5, 1656. https://doi.org/10.3390/rs12101656

[8] P. Li, D. Liu, X. Xia, and S. Baldi, Adardupilot: An ardupilot compatible adaptive autopilot, *IFAC-PapersOnLine*, **56** (2023), no. 1, 8097-8104. https://doi.org/10.1016/j.ifacol.2023.10.964

[9] W. Li, D. Wang, M. Li, Y. Gao, J. Wu, and X. Yang, Field detection of tiny pests from sticky trap images using deep learning in agricultural greenhouse, *Computers and Electronics in Agriculture*, **183** (2021), no. 4, 106048. https://doi.org/10.1016/j.compag.2021.106048

[10] Z. Liu, S. Dhamankar, J. Evans, C. Allen, C. Jiang, G. Shaver, A. Etienne, T. Vyn, C. Puryk, and B. McDonald, Automation of agricultural grain unloading-on-the-go, *IFAC-PapersOnLine*, **55** (2022), no. 10, 248-253. https://doi.org/10.1016/j.ifacol.2022.10.292

[11] J. Malaguit, V. M. Mendoza, J. Tubay, and M. Mata, Identifying patterning behavior in a plant infestation of insect pests, *Mathematical Biosciences*, **362** (2023) no. 6, 109032.
https://doi.org/10.1016/j.mbs.2023.109032

[12] R. Nidamanuri, R. Jayakumari, and R. Anandakumar, Object-level classification of vegetable crops in 3D lidar point cloud using deep learning convolutional neural networks, *Precision Agriculture*, **22** (2021), no. 10.
https://doi.org/10.1007/s11119-021-09803-0

[13] T. Poblete, J. Navas Corts, A. Hornero, C. Camino, R. Caldern Madrid, R. Hernandez Clemente, B. Landa, and P. Zarco-Tejada, Detection of symptoms induced by vascular plant pathogens in tree crops using high-resolution satellite data: Modelling and assessment with airborne hyperspectral imagery, *Remote Sensing of Environment*, **295** (2023), no. 9, 113698. https://doi.org/10.1016/j.rse.2023.113698

[14] C. Prakash, L.P. Singh, A. Gupta, and S.K. Lohan, Advancements in smart farming: A comprehensive review of IoT, wireless communication, sensors, and hardware for agricultural automation, *Sensors and Actuators A: Physical*, **362** (2023), 114605.
https://doi.org/10.1016/j.sna.2023.114605

[15] M. Prez-Ruiz, D. Slaughter, C. Gliever, and S. Upadhyaya, Tractor- based real-time kinematic-global positioning system (RTK-GPS) guidance system for geospatial mapping of row crop transplant, *Biosystems Engineering*, **111** (2012) no. 1, 64-71.
https://doi.org/10.1016/j.biosystemseng.2011.10.009

[16] R. Raja, D. Slaughter, S. Fennimore, T. Nguyen, V. Vuong, N. Sinha, L. Tourte, R. Smith, and M. Siemens, Crop signalling: A novel crop recognition technique for robotic weed control sciencedirect, *Biosystems Engineering*, **187** (2019), no. 11, 278-291.
https://doi.org/10.1016/j.biosystemseng.2019.09.011

[17] M. Roznik, M. Boyd, and L. Porth, Improving crop yield estimation by applying higher resolution satellite NDVI imagery and high-resolution cropland masks, *Remote Sensing Applications: Society and Environment*, **25** (2022), no. 1, 100693. https://doi.org/10.1016/j.rsase.2022.100693

[18] R. Sanz, J. Llorens Calveras, A. Escol, J. Arn, M. Ribes-Dasi, J. Masip-Vilalta, F. Camp, F. Grcia-Aguil, F. Solanelles, S. Planas de Mart, T. Pallej, J. Palacin-Roca, E. Gregorio Lopez, I. Del-Moral-Martnez, and J. Rosell-Polo, Innovative LIDAR 3D dynamic measurement system

to es- timate fruit-tree leaf area, *Sensors*, **11** (2011), no. 12, 5769-91. https://doi.org/10.3390/s110605769

[19] U.A Schneider, P. Havlk, E. Schmid, H. Valin, A. Mosnier, M. Obersteiner, H. Bttcher, R. Skalsk, J. Balkovi, T. Sauer, and S. Fritz, Impacts of population growth, economic development, and technical change on global food production and consumption, *Agricultural Systems*, **104** (2011), no. 2, 204-215. https://doi.org/10.1016/j.agsy.2010.11.003

[20] D. Shanmugavel, I. Rusyn, O. Solorza-Feria, and S.-K. Kamaraj, Sustainable SMART fertilizers in agriculture systems: A review on fundamentals to in-field applications, *Science of The Total Environment*, **904** (2023), 166729. https://doi.org/10.1016/j.scitotenv.2023.166729

[21] M. Zanella, R. Martins, F. Silva, L. Carvalho, M. Alves, and J. Fim Rosas, Coffee yield prediction using high-resolution satellite imagery and crop nutritional status in southeast Brazil, *Remote Sensing Applications: Society and Environment*, **33** (2023), no. 11, 101092. https://doi.org/10.1016/j.rsase.2023.101092

Received: December 7, 2023; Published: December 23, 2023